

Dynamical characterization of topological phases beyond the minimal modelsXi Wu^{Ⓧ,*}, Panpan Fang^{Ⓧ,†} and Fuxiang Li[‡]*School of Physics and Electronics, Hunan University, Changsha 410082, China* (Received 1 March 2023; accepted 14 April 2023; published 15 May 2023)

Dynamical characterization of topological phases under quantum quench dynamics has been demonstrated as a powerful and efficient tool. Previous studies have focused on systems of which the Hamiltonian consists of matrices that commute with each other and satisfy Clifford algebra. In this work we consider the characterization of topological phases with Hamiltonians that are beyond the minimal model. Specifically, the quantum quench dynamics of two types of layered systems is studied, which consist of matrices of Hamiltonians that do not all satisfy Clifford algebra. We find that the terms which anticommute with others can hold common band-inversion surfaces, which controls the topology of all the bands, but for other terms, there is no universal behavior and they need to be treated case by case.

DOI: [10.1103/PhysRevA.107.052209](https://doi.org/10.1103/PhysRevA.107.052209)**I. INTRODUCTION**

Topological phases of matter were originally defined in equilibrium in terms of topological invariants by the bulk Hamiltonian in momentum space or by the number of edge states on the boundary of the material [1,2]. These two approaches are related to each other by the so-called bulk-edge correspondence [3,4]. In recent years, the bulk-edge correspondence has been generalized to the so-called bulk-edge-hinge (corner) correspondence, in which the states localized on the intersection of two boundaries are protected by the topology of the material. Such topological phases are called higher-order topological insulators [5,6]. Meanwhile, many studies show that the topological structure of a system can also be probed by nonequilibrium quench dynamics in both theory [7–12] and experiment [13–18]. Specifically, a different kind of bulk-edge correspondence, based on nonequilibrium dynamics, has been proposed by Liu and co-workers through the so-called dynamical spin-texture fields on the band-inversion surfaces (BISs) in time-averaged spin polarization (TASP). It has been formulated in theory [19–21] and realized in the experiment [22,23]. Later, it was generalized to Floquet systems [24] and higher-order topological insulators [25]. Compared with traditional equilibrium approaches, the method of Liu and co-workers not only shows band topology from a different angle, but also has high feasibility and experimental accuracy.

However, most of the nonequilibrium approaches carried out so far on topological systems have focused on simple models like the Su-Schrieffer-Heeger model [26] and Haldane model (or Chern insulator) [27]. The studies of Liu and co-workers also only consider examples of minimal models in which the Hamiltonians can be expanded in terms of Γ matrices, all satisfying Clifford algebra. In such minimal models,

the topological invariant of the band can be expressed by the coefficient of the Γ matrices in a very simple way and therefore BISs and spin-texture fields appear in a natural way. One way of extending the minimal model is in the higher-order topological insulators by the nested configurations of the BIS [25,28]. It was mentioned that models beyond the minimal model are possible in such models. However, one still wonders how far the procedure of the minimal model can be applied in the case of generic multiband Hamiltonians.

In this paper we generalize the idea of Liu and co-workers and consider systems that are beyond their minimal models. In these systems, the Hamiltonians are expanded by matrices that do not satisfy Clifford algebra: Some terms anticommute with others but some do not. Specifically, we consider layered systems with the same type of layer but with two different types of stacking, giving rise to two different topological structures [29–32]. Though these models have some similarities to minimal models, they are more general. One of them, $AB - BA$ stacking, can be block diagonalized and therefore can be separated into subsystems, i.e., minimal models, but the other one, BA stacking, cannot.

We describe the quench dynamics of the layered systems and characterize the topology of these systems. Our findings are as follows. The terms which anticommute with others can hold a common BIS and control the topology of all the bands without referring to the information of other terms. However, with the band dispersion considered, the condition for a term to have a BIS is relaxed as follows: If it is nonzero at all momentum values, it can keep the gap open for any deformation of the other terms. This holds for both $AB - BA$ stacking and BA stacking systems. Inside the subsystems of $AB - BA$ stacking, there exist BISs that control the topology of the subsystems. In order to clarify the whole topological number, these subsystems need to be treated separately. The BA stacking systems need to be treated as a whole. In addition, the interlayer hopping can also be obtained from the TASP itself in these two stacking systems.

The paper is organized as follows. In Sec. II we introduce two stacking types of layered systems, $AB - BA$ and

*wuxi5949@hnu.edu.cn

†f2p@hnu.edu.cn

‡fuxiangli@hnu.edu.cn

BA stacking, and their topology. In Sec. III we show the way to quench the system and characterize topology for bilayer systems, providing the essence of the method. In Sec. IV we generalize the results into multilayer systems, showing this method to be generically useful. In Sec. V we summarize and discuss possible future directions.

II. LAYERED SYSTEMS

In this section we introduce the layered systems and discuss their band topology. First, we consider the following Hamiltonian for the monolayer system:

$$H_1 = \begin{bmatrix} h_3 & h_1 - ih_2 \\ h_1 + ih_2 & -h_3 \end{bmatrix}. \quad (1)$$

This Hamiltonian can describe interactions within two spin- $\frac{1}{2}$ states such as the Qi-Wu-Zhang model [33] or sublattice degrees of freedom such as the Haldane model [27]. Then the two types of layered systems can be given. One is the *AB* – *BA* stacking system, which means that the interlayer hopping has the direction both from the *A* of the first layer to the *B* of the second layer and from the *B* of the first layer to the *A* of the second layer. The other is the *BA* stacking system, which means that the interlayer hopping is only from the *B* of the first layer to the *A* of the second layer (*AB* stacking system has the same spectrum). For convenience, we leave all the details of the derivation to the Appendixes.

A. The *AB* – *BA* stacking system

The bilayer *AB* – *BA* stacking system is defined as

$$H_{AB-BA}^2 = \begin{bmatrix} h_3 & h_1 - ih_2 & & t \\ h_1 + ih_2 & -h_3 & t & \\ & t & h_3 & h_1 - ih_2 \\ t & & h_1 + ih_2 & -h_3 \end{bmatrix} \\ = \sum_{i=1}^3 h_i \mathbb{1} \otimes \sigma_i + t \sigma_1 \otimes \sigma_1, \quad (2)$$

where t is the interlayer hopping amplitude. The schematic diagram of this bilayer system is shown in Fig. 1. The energy spectrum is

$$E_I^\pm = \pm \sqrt{(h_1 + t)^2 + h_2^2 + h_3^2} = \pm E_I, \\ E_{II}^\pm = \pm \sqrt{(h_1 - t)^2 + h_2^2 + h_3^2} = \pm E_{II}. \quad (3)$$

The Chern number of this bilayer system is the sum of the Chern numbers of the two subsystems *I* and *II* (for details, see Appendix C). As shown in Fig. 2(a), we plot the phase diagram of the above bilayer system. One can see the following from the phase diagram. (i) If the monolayer system H_1 is topologically trivial, the *AB* – *BA* stacking system remains trivial for all t . (ii) If the monolayer model H_1 is topologically nontrivial, the *AB* – *BA* stacking system will undergo a phase transition by tuning t at a finite m . The phase transitions happen at (t, m) such that $h_1 \pm t = h_2 = h_3 = 0$. Thus, in order to focus on the effect of interlayer hopping on the layered systems, H_1 is always assumed to be topological in the following.

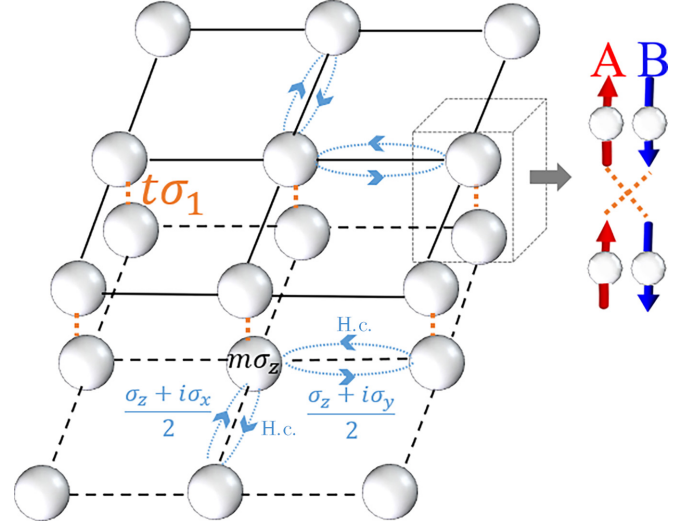


FIG. 1. Lattice realization of H_{AB-BA}^2 on a square bilayer lattice, in which up and down spins represent *A* and *B* degrees of freedom, respectively. The monolayer Hamiltonian is from the Qi-Wu-Zhang model, in which $h_1 = \sin k_x$, $h_2 = \sin k_y$, and $h_3 = m - \cos k_x - \cos k_y$.

The *AB* – *BA* stacking multilayer models has the Hamiltonian

$$H_{AB-BA}^N = \begin{bmatrix} \sum_{i=1}^3 h_i \sigma_i & t \sigma_1 & & \\ t \sigma_1 & \sum_{i=1}^3 h_i & t \sigma_1 & \\ & t \sigma_1 & \sum_{i=1}^3 h_i & \dots \\ & & \dots & \dots \end{bmatrix} \quad (4)$$

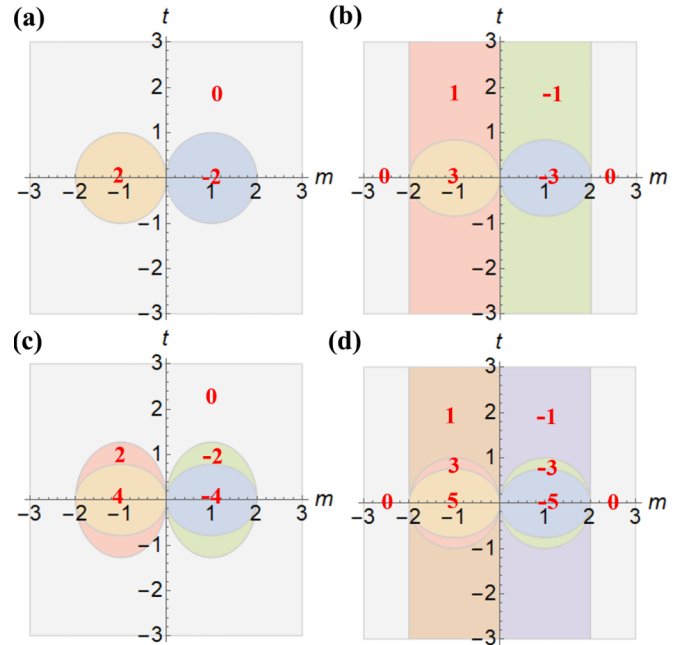


FIG. 2. Phase diagrams of H_{AB-BA}^N with $h_1 = \sin k_x$, $h_2 = \sin k_y$, and $h_3 = m - \cos k_x - \cos k_y$. The number of layers N is (a) 2, (b) 3, (c) 4, and (d) 5. The numbers marked in red denote the topological numbers in the corresponding regions.

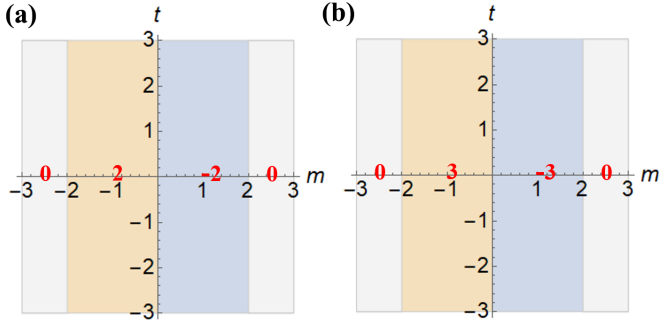


FIG. 4. Phase diagrams of H_{BA}^2 and H_{BA}^3 with $h_1 = \sin k_x$, $h_2 = \sin k_y$, and $h_3 = m - \cos k_x - \cos k_y$. The numbers marked in red denote the topological numbers in the corresponding regions.

quench dynamics. Unlike the minimal models, not all the terms in the Hamiltonian of layered systems satisfy Clifford algebra and there is no standard mapping of the coefficients h_i of these terms onto an effective field as in the two-level system. Therefore, the BIS, which emerges on the TASP, should be carefully defined. For simplicity, we use the Hamiltonian of the Qi-Wu-Zhang model for the Hamiltonian of the monolayer model for the density plots in this section.

A. Common BISs

In the case of layered systems, the Clifford algebra is not satisfied for all terms in the Hamiltonian except a special term $h_3 \mathbb{1} \otimes \sigma_3$. The term $h_3 \mathbb{1} \otimes \sigma_3$ anticommutes with all other terms and can be used to define the common BIS in the $AB - BA$ stacking model as well as the bilayer BA stacking model. The process is as follows.

First, we prepare an initial state as

$$\begin{aligned} \rho_0 &= \frac{\mathbb{1}}{2} \otimes \frac{1}{2}(\mathbb{1} - \sigma_3) = \frac{1}{2} \begin{bmatrix} 1 & 0 \\ 0 & 1 \end{bmatrix} \otimes \begin{bmatrix} 0 & 0 \\ 0 & 1 \end{bmatrix} \\ &= \frac{1}{2} \begin{bmatrix} 0 & 0 & 0 & 0 \\ 0 & 1 & 0 & 0 \\ 0 & 0 & 0 & 0 \\ 0 & 0 & 0 & 1 \end{bmatrix}, \end{aligned} \quad (10)$$

which is a mixed state of two eigenstates of the prequench Hamiltonian $H_0 = h_3 \mathbb{1} \otimes \sigma_3$ with the same eigenvalue. Then we can suddenly quench H_0 into the postquench Hamiltonian H_2 , which may be H_{AB-BA}^2 or H_{BA}^2 . After a long time of unitary evolution, we can obtain the corresponding TASP

$$\overline{\langle \mathbb{1} \otimes \sigma_i \rangle_{\rho_0}} = -h_3 \sum_m \frac{\langle \tilde{\psi}_m | \mathbb{1} \otimes \sigma_i | \tilde{\psi}_m \rangle}{4E_m}, \quad (11)$$

where $|\tilde{\psi}_m\rangle$ and E_m are the normalized eigenvector and the eigenvalue of the postquench Hamiltonian at the m th level, respectively (see Appendix E for the derivation).

Thus, the BIS, where all the components of TASP vanish, can be identified at the region with momentum points

$$\mathcal{B} = \{\mathbf{k} | \overline{\langle \mathbb{1} \otimes \vec{\sigma} \rangle_{\rho_0}} = 0\}. \quad (12)$$

Alternatively, from the perspective of the Hamiltonian, the BIS is at the region with momentum points where $h_3 = 0$, which is consistent with the definition of the BIS in Ref. [19].

In particular, we have

$$\overline{\langle \mathbb{1} \otimes \sigma_3 \rangle_{\rho_0}} = -h_3^2 \sum_m \frac{1}{4E_m^2}. \quad (13)$$

Let us explain the condition for BISs. As long as there is some $h_i \neq 0$ in the whole Brillouin zone which keeps the gap open regardless of other terms, we can continuously deform the Hamiltonian into $H = h_i \mathbb{1} \otimes \sigma_i$, which is a trivial one, so the disappearance of the BIS means that the postquench Hamiltonian is topologically trivial. However, when there is a BIS appearing (or the surface where $h_i = 0$) we are not allowed to deform Hamiltonian freely to $H = h_i \mathbb{1} \otimes \sigma_i$; therefore, this may mean that the postquench Hamiltonian is topological. As one can see from Eqs. (3), (5), (7), and (9), E^2 is the sum of h_3^2 and other positive terms (see [34] for a general proof), so h_3 satisfies this condition quite obviously. Of course, in order to know whether the system is truly topological we need to consider further information of the dynamical topological invariants, which is explained in the rest of this section. Thus, this BIS is as powerful as the one in the minimal models like the monolayer system H_1 in (1) for the characterization of bulk topology. Here we need to emphasize that this special term $h_3 \mathbb{1} \otimes \sigma_3$ that anticommutes with all other terms is a sufficient condition for having a BIS, but not a necessary one. As we will see in the following sections, for other terms that do not anticommute with all other terms, the characterization procedure depends very much on the energy spectrum considered. To be specific, for the $AB - BA$ stacking model, $h_1 \pm t$ and h_2 satisfy the condition for defining the BIS while for the BA stacking model h_1 and h_2 satisfy the condition above.

B. Dynamical characterization in the $AB - BA$ stacking system

In this section we show how to capture the bulk topology of the postquench Hamiltonian of the bilayer $AB - BA$ system. Starting from $\rho_0 = \frac{1}{2} \otimes \frac{1}{2}(\mathbb{1} - \sigma_j)$, $j = 1, 2, 3$, a mixed eigenstate of the Hamiltonian $H_0 = h_j \mathbb{1} \otimes \sigma_j$, we suddenly quench the Hamiltonian H_0 into H_{AB-BA}^2 in (2). Then the exact form of TASP can be obtained as

$$\overline{\langle \mathbb{1} \otimes \sigma_i \rangle_{\rho_0}} = -\frac{h_i^i h_I^j}{2E_I^2} - \frac{h_{II}^i h_{II}^j}{2E_{II}^2}, \quad i = 1, 2, 3, \quad (14)$$

in which $h_i^1 = h_1 + t$, $h_i^2 = h_2$, $h_i^3 = h_3$, $h_{II}^1 = h_1 - t$, $h_{II}^2 = h_2$, and $h_{II}^3 = h_3$.

However, Eq. (14) gives the overlap between two topological structures, namely, the BISs and the dynamical spin-texture fields. The BISs can be defined for h_2 and h_3 but not for h_1 . Therefore, in order to show the topological information independently, we consider splitting the TASP in (14) into two subspaces.

By defining $\mathcal{D}_{\pm} = \frac{1}{2}(\mathbb{1} \pm \sigma_1)$, we obtain the long-time average of the operators $\mathcal{O}_I^i = 2\mathcal{D}_+ \otimes \sigma_i$ and $\mathcal{O}_{II}^i = 2\mathcal{D}_- \otimes \sigma_i$, which we call generalized time-averaged spin polarization (GTASP) hereafter, as follows:

$$\overline{\langle \mathcal{O}_I^i \rangle_{\rho_0}} = -\frac{h_i^i h_I^j}{E_I^2}, \quad (15)$$

$$\overline{\langle \mathcal{O}_{II}^i \rangle_{\rho_0}} = \frac{h_{II}^i h_{II}^j}{E_{II}^2}. \quad (16)$$

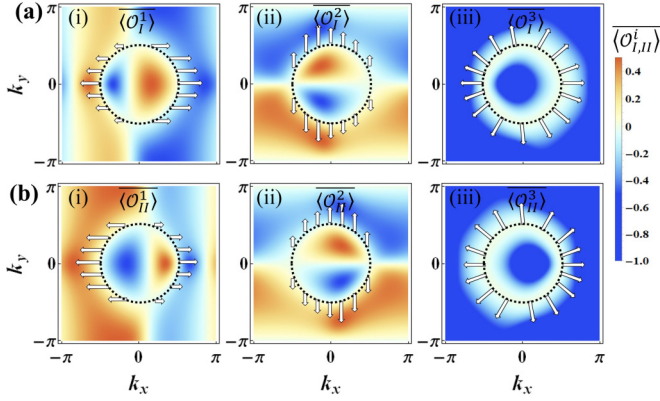


FIG. 5. (a) The GTASP and topological characterization of H_I . (b) The GTASP and topological characterization of H_{II} . Here $m = 1$, $t = 0.4$, and $\rho_0 = \frac{1}{2} \otimes \frac{1}{2} (\mathbb{1} - \sigma_3)$. The common rings emergent in (a) and (b) are the so-called BISs. Along the BISs the winding of dynamical fields $\widetilde{\mathbf{g}}_I$ and $\widetilde{\mathbf{g}}_{II}$ give a nontrivial topological number -1 . The white arrows represent the two components of (a i) and (a ii) $\widetilde{\mathbf{g}}_I$ and (b i) and (b ii) $\widetilde{\mathbf{g}}_{II}$ and linear combinations of the components (a iii) $\widetilde{\mathbf{g}}_I$ and (b iii) $\widetilde{\mathbf{g}}_{II}$.

At this time, the two BISs are well defined and identified in the corresponding subspace:

$$\mathcal{B}_I = \{\mathbf{k} | \langle \overline{\mathcal{O}}_I \rangle_{\rho_0} = 0\}, \quad (17)$$

$$\mathcal{B}_{II} = \{\mathbf{k} | \langle \overline{\mathcal{O}}_{II} \rangle_{\rho_0} = 0\}. \quad (18)$$

Then, after measuring the corresponding dynamical spin-texture fields, i.e., gradient fields of GTASP, on \mathcal{B}_I and \mathcal{B}_{II} , we can easily characterize the bulk topology of the system. The gradient fields in two subspaces are

$$\widetilde{g}_I^i(\mathbf{k}) = -\frac{1}{\mathcal{N}_{\mathbf{k}}} \partial_{k_{\perp}} \langle \overline{\mathcal{O}}_I^i \rangle_{\rho_0}. \quad (19)$$

$$\widetilde{g}_{II}^i(\mathbf{k}) = -\frac{1}{\mathcal{N}_{\mathbf{k}}} \partial_{k_{\perp}} \langle \overline{\mathcal{O}}_{II}^i \rangle_{\rho_0}. \quad (20)$$

Here k_{\perp} is perpendicular to the $\mathcal{B}_{I,II}$ and $\mathcal{N}_{\mathbf{k}}$ is the normalization factor. After some algebra, we arrive at

$$\widetilde{g}_I^i(\mathbf{k}) \Big|_{\mathbf{k} \in \mathcal{B}_I} = \frac{h_I^i(0, \mathbf{k}_{\parallel})}{\sum_{i \neq j} [h_I^i(0, \mathbf{k}_{\parallel})]^2} = \widehat{h}_I^{so,i}, \quad (21)$$

$$\widetilde{g}_{II}^i(\mathbf{k}) \Big|_{\mathbf{k} \in \mathcal{B}_{II}} = \frac{h_{II}^i(0, \mathbf{k}_{\parallel})}{\sum_{i \neq j} [h_{II}^i(0, \mathbf{k}_{\parallel})]^2} = \widehat{h}_{II}^{so,i}. \quad (22)$$

Here both $\widetilde{\mathbf{g}}_I$ and $\widetilde{\mathbf{g}}_{II}$ are vectors with two components. If we choose the initial state $\rho_0 = \frac{1}{2} \otimes \frac{1}{2} (\mathbb{1} - \sigma_3)$, $\widetilde{\mathbf{g}}_I = \widehat{\mathbf{h}}_I^{so} = (\widehat{h}_I^1, \widehat{h}_I^2)$ and $\widetilde{\mathbf{g}}_{II} = \widehat{\mathbf{h}}_{II}^{so} = (\widehat{h}_{II}^1, \widehat{h}_{II}^2)$.

The bulk topological number can be obtained by the sum of the dynamical invariants defined in each subspace along the BISs,

$$w = w_I + w_{II} = \frac{1}{2\pi} \left(\int_{\mathcal{B}_I} \widetilde{\mathbf{g}}_I d\widetilde{\mathbf{g}}_I + \int_{\mathcal{B}_{II}} \widetilde{\mathbf{g}}_{II} d\widetilde{\mathbf{g}}_{II} \right). \quad (23)$$

As shown in Figs. 5(a) and 5(b), we plot the GTASP of H_I and H_{II} , respectively, for the case when the Chern number is -2 for the initial state $\rho_0 = \frac{1}{2} \otimes \frac{1}{2} (\mathbb{1} - \sigma_3)$. On the black

dashed ring, all the components of GTASP vanish and thus we identify it as $\mathcal{B}_{I,II}$. The gradient fields $\widetilde{g}_{I,II}(\mathbf{k})$ (arrows) plotted along the BISs show topological number -1 for each subspace. The bilayer system with a topological number -2 is successfully characterized. In addition, using $h_j^1 = h_1(\mathbf{k}) + t = 0$, we can obtain t as $-h^1(\mathbf{k}|_{h_j^1=0})$. This correspond to the white line across the BIS in Fig. 5(ai). Obviously, if the white line across the BIS disappears, meaning $h_j^1 \neq 0$ anywhere in the Brillouin zone, the model is topologically trivial (see Appendix A).

C. Dynamical characterization in the BA stacking system

The BA bilayer system is not a minimal model nor can it be block diagonalized in a simple way, meaning there is no independent subsystem as in minimal models, so there is no simple way to calculate the Chern number directly. Similar to the preceding section, for initial state $\rho_0 = \frac{1}{2} \otimes \frac{1}{2} (\mathbb{1} - \sigma_j)$, $j = 1, 2, 3$, we can obtain the TASP of bilayer system H_{BA}^2 as

$$\langle \mathbb{1} \otimes \sigma_i \rangle_{\rho_0} = -h_i h_j A_{ij}, \quad (24)$$

in which A_{ij} are coefficients and there is no summation over i and j . Here we fortunately find that the zeros of TASP remain the same as the monolayer model. The reason is that t does not induce the gap closing, so the topological structure remains the same. Thus the BIS can be defined following the original minimal model:

$$\mathcal{B} = \{\mathbf{k} | \langle \mathbb{1} \otimes \overline{\sigma} \rangle_{\rho_0} = 0\}. \quad (25)$$

One may wonder that why BISs still work for terms like $h_1 \mathbb{1} \otimes \sigma_1$ and $h_2 \mathbb{1} \otimes \sigma_2$ that do not anticommute with all other terms. The reason can be seen in the dispersions (7) and (9): When we keep the condition, for instance, $h_1 \neq 0$ throughout the Brillouin zone, the gap is not closed as we continuously deform the Hamiltonian into $H = h_1 \mathbb{1} \otimes \sigma_1$, which is a trivial one, and this shows that the original Hamiltonian is topologically trivial. Moreover, this condition works for all the BISs in $AB - BA$ systems as well. Therefore, this condition is necessary for a BIS to be useful for the models being considered in this paper.

Next we measure the dynamical spin-texture fields on the BIS, which can be obtained from the gradient of TASP

$$\widetilde{g}_i(\mathbf{k}) = -\frac{1}{\mathcal{N}_{\mathbf{k}}} \partial_{k_{\perp}} \langle \mathbb{1} \otimes \sigma_i \rangle_{\rho_0}, \quad (26)$$

in which the difference is calculated as

$$\Delta \langle \mathbb{1} \otimes \sigma_i \rangle_{\rho_0} \Big|_{k_{\perp} \rightarrow 0} \propto -2(A_{ij} h_j) |_{(0, \mathbf{k}_{\parallel})} k_{\perp}. \quad (27)$$

Thus,

$$\widetilde{g}_p(\mathbf{k}) \Big|_{\mathbf{k} \in \mathcal{B}} = \frac{A_{pj} h_p}{(A_{pj} h_p)^2 + (A_{qj} h_q)^2}, \quad (28)$$

with $p \neq q \neq j$ and $p, q, j = 1, 2, 3$. Specifically, if we choose the initial state $\rho_0 = \frac{1}{2} \otimes \frac{1}{2} (\mathbb{1} - \sigma_3)$, \widetilde{g}_1 and \widetilde{g}_2 are equal to $\frac{A_{13} h_1}{(A_{13} h_1)^2 + (A_{23} h_2)^2}$ and $\frac{A_{23} h_2}{(A_{23} h_2)^2 + (A_{13} h_1)^2}$, respectively. Although there is a rescaling in \widetilde{g}_i , it does not change the bulk topology. The topological number should be given by the

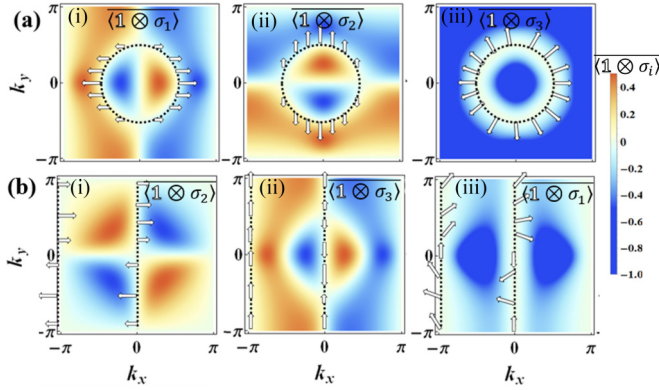


FIG. 6. The TASP and topological characterization of H_{BA}^2 . Here $m = 1$ and $t = 0.4$. The initial state ρ_0 is (a) $\frac{1}{2} \otimes \frac{1}{2}(\mathbb{1} - \sigma_3)$ and (b) $\frac{1}{2} \otimes \frac{1}{2}(\mathbb{1} - \sigma_1)$. The white arrows represent (a i), (a ii), (b i), and (b ii) the two components of \tilde{g} and (a iii) and (b iii) \tilde{g} as a linear combination of the components.

winding of the dynamical field on the BIS

$$w = \frac{2}{2\pi} \left(\int_{\mathcal{B}} \tilde{\mathbf{g}} d\tilde{\mathbf{g}} \right). \quad (29)$$

The TASP of the BA stacking system does not reflect the exact value of the Chern number, but only reflects whether the system is topological. However, since the only missing information is related to the number of layers, which is 2, we just added it as a coefficient by hand in the definition of w .

As shown in Figs. 6(a) and 6(b), we plot the TASP of the bilayer BA stacking system for the case when the Chern number is -2 for $\rho_0 = \frac{1}{2} \otimes \frac{1}{2}(\mathbb{1} - \sigma_3)$ and $\rho_0 = \frac{1}{2} \otimes \frac{1}{2}(\mathbb{1} - \sigma_1)$, respectively. On dashed curves, all the components of TASP vanish and thus we identify it as a BIS. The gradient fields $g(\mathbf{k})$ (arrows) plotted along the BISs show topological number -2 .

In addition, as shown in Fig. 7, taking the initial state $\rho_0 = \frac{1}{2} \otimes \frac{1}{2}(\mathbb{1} - \sigma_3)$ as an example, we plot the component of TASP $\overline{\langle \mathbb{1} \otimes \sigma_1 \rangle}_{\rho_0}$ with different interlayer hopping t . When increasing the interlayer hopping t , the maximum value of TASP decreases and thus we can obtain the value of the interlayer hopping t by the variation of the amplitude of TASP as shown in Fig. 8. If we choose the monolayer model as the Haldane model, the results will be similar (see Appendix B).

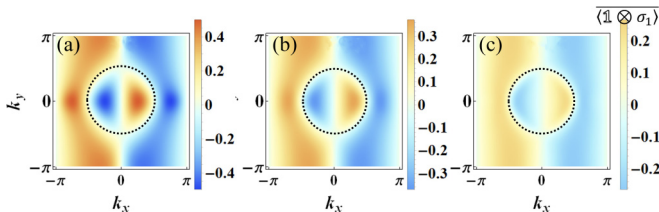


FIG. 7. Component of TASP $\overline{\langle \mathbb{1} \otimes \sigma_1 \rangle}_{\rho_0}$ of H_{BA}^2 for different values of interlayer hopping t : (a) $t = 0$, (b) $t = 0.9$, and (c) $t = 1.8$.

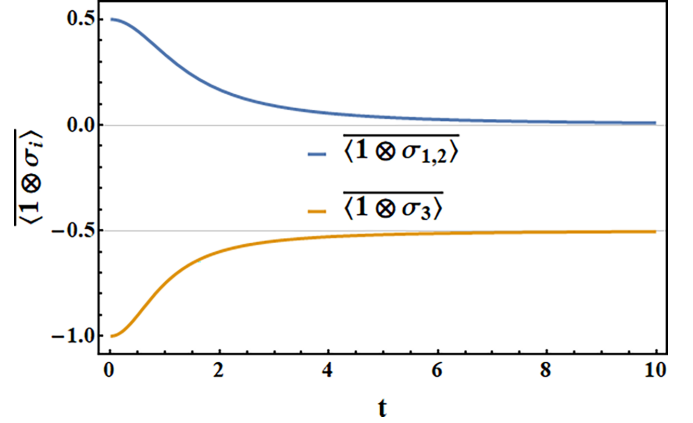


FIG. 8. Relation between the TASP $\overline{\langle \mathbb{1} \otimes \sigma_i \rangle}_{\rho_0}$ and interlayer hopping t . We choose the momentum points, at which the corresponding components of the TASP have the maximum absolute value when $t = 0$, to show the specific relation between the components of the TASP and interlayer hopping t . Specifically, in $\overline{\langle \mathbb{1} \otimes \sigma_1 \rangle}_{\rho_0}$, $\overline{\langle \mathbb{1} \otimes \sigma_2 \rangle}_{\rho_0}$, and $\overline{\langle \mathbb{1} \otimes \sigma_3 \rangle}_{\rho_0}$, we choose the momentum points $(\frac{\pi}{4}, 0)$, $(0, \frac{\pi}{4})$, and $(0, 0)$, respectively. At the momentum points $(\frac{\pi}{4}, 0)$ and $(0, \frac{\pi}{4})$, both $\overline{\langle \mathbb{1} \otimes \sigma_1 \rangle}_{\rho_0}$ and $\overline{\langle \mathbb{1} \otimes \sigma_2 \rangle}_{\rho_0}$ are equal to $\frac{1}{2+t^2}$. At the momentum point $(0, 0)$, $\overline{\langle \mathbb{1} \otimes \sigma_3 \rangle}_{\rho_0}$ is equal to $\frac{2+t^2}{2+2t^2}$.

IV. DYNAMICAL CHARACTERIZATION IN THE MULTILAYER SYSTEM

In this section we discuss the situation in the system with more than two layers. The common BIS is the same as in Sec. III A except that we need to replace $\rho_0 = \frac{1}{2} \otimes \frac{1}{2}(\mathbb{1} - \sigma_3)$ by $\rho_0 = \frac{1}{N} \otimes \frac{1}{2}(\mathbb{1} - \sigma_3)$, so we are not going to repeat the discussion here. The other parts of the discussion in Sec. III can be easily generalized in the following sections.

A. Dynamical characterization in the multilayer $AB - BA$ stacking system

For an N -layer $AB - BA$ stacking system, there is a way to quench the subsystems independently too. The procedure is parallel to the bilayer case. Starting from $\rho_0 = \frac{1}{N} \otimes \frac{1}{2}(\mathbb{1} - \sigma_j)$, $j = 1, 2, 3$, a mixed eigenstate of the Hamiltonian $H_0 = h_j \mathbb{1} \otimes \sigma_j$, we quench the Hamiltonian into H_{AB-BA}^N in Eq. (4). The TASP is

$$\overline{\langle \mathbb{1} \otimes \sigma_i \rangle}_{\rho_0} = - \sum_{r=1}^N \frac{h_r^i h_r^j}{2E_r^2}. \quad (30)$$

The result of TASP in Eq. (30) gives the overlap of N topological structures. Instead we find the GTASP

$$\overline{\langle \mathbf{a}_r \mathbf{a}_r^T \otimes \sigma_i \rangle}_{\rho_0} = - \frac{h_r^i h_r^j}{E_r^2}, \quad (31)$$

in which $\mathbf{a}_r = \sqrt{\frac{2}{N+1}} (\sin \theta_r, \sin 2\theta_r, \dots, \sin N\theta_r)^T$, $h_r^1 = h_1 - 2t \cos \theta_r$, $h_r^2 = h_2$, and $h_r^3 = h_3$, with $\theta_r = \frac{r\pi}{N+1}$ and $r = 1, 2, \dots, N$. Each set of $\mathbf{a}_r \mathbf{a}_r^T \otimes \sigma_1$, $\mathbf{a}_r \mathbf{a}_r^T \otimes \sigma_2$, and $\mathbf{a}_r \mathbf{a}_r^T \otimes \sigma_3$

exists in a subspace that is orthogonal to others and the GTASP can characterize the topology of each subspace. The BIS in each subspace is written as

$$\mathcal{B}_r = \{\mathbf{k} | \overline{\langle \mathbf{a}_r \mathbf{a}_r^T \otimes \sigma_i \rangle}_{\rho_0} = 0\} \quad (32)$$

or \mathcal{B}_r is at the region where $h_r^j = 0$. The dynamical spin-texture fields in each subspace can also be obtained by calculating

$$\widetilde{g}_r^i(\mathbf{k}) = -\frac{1}{\mathcal{N}_{\mathbf{k}}} \partial_{k_{\perp}} \overline{\langle \mathbf{a}_r \mathbf{a}_r^T \otimes \sigma_i \rangle}_{\rho_0}. \quad (33)$$

After some algebra, we get

$$\widetilde{g}_r^i(\mathbf{k}) \Big|_{\mathbf{k} \in \mathcal{B}_r} = \frac{h_r^i(0, \mathbf{k}_{\parallel})}{\sum_{i \neq j} [h_r^i(0, \mathbf{k}_{\parallel})]^2} = \hat{h}_r^{so,i}. \quad (34)$$

In addition, the bulk topological number is the sum of the dynamical invariants defined in the subspaces as

$$w = \sum_{r=1}^N w_r = \sum_{r=1}^N \frac{1}{2\pi} \int_{\mathcal{B}} \widetilde{\mathbf{g}}_r \cdot d\widetilde{\mathbf{g}}_r. \quad (35)$$

B. Dynamical characterization in the multilayer BA stacking system

Following the same procedure as in Sec. III C, starting from $\rho_0 = \frac{\mathbb{1}}{N} \otimes \frac{1}{2}(\mathbb{1} - \sigma_j)$, $j = 1, 2, 3$, we quench the Hamiltonian into H_{BA}^N and then obtain the TASP. After some algebra, we have

$$\overline{\langle \mathbb{1} \otimes \sigma_i \rangle}_{\rho_0} = -h_i h_j A_{ij}^{(N)}, \quad (36)$$

in which there is no summation over i and j . The $A_{ij}^{(N)}$ are the coefficients that depend on the numbers of layers. Like the bilayer BA stacking system, the BIS can be defined as

$$\mathcal{B} = \{\mathbf{k} | \overline{\langle \mathbb{1} \otimes \vec{\sigma} \rangle}_{\rho_0} = 0\}. \quad (37)$$

Let us look at the dynamical spin-texture fields

$$\widetilde{g}_i(\mathbf{k}) = -\frac{1}{\mathcal{N}_{\mathbf{k}}} \partial_{k_{\perp}} \overline{\langle \mathbb{1} \otimes \sigma_i \rangle}_{\rho_0}. \quad (38)$$

For the initial state

$$\rho_0 = \frac{\mathbb{1}}{N} \otimes \frac{1}{2}(\mathbb{1} - \sigma_j),$$

whose BIS is at $h_j = 0$, the difference is calculated as

$$\Delta \overline{\langle \mathbb{1} \otimes \sigma_i \rangle}_{\rho_0} \Big|_{k_{\perp} \rightarrow 0} \propto -2(A_{ij}^{(N)} h_{so,i}) \Big|_{(0, \mathbf{k}_{\parallel})} k_{\perp}. \quad (39)$$

Thus,

$$\widetilde{g}_p(\mathbf{k}) \Big|_{\mathbf{k} \in \mathcal{B}} = \frac{A_{pj}^{(N)} h_p}{(A_{pj}^{(N)} h_p)^2 + (A_{qj}^{(N)} h_q)^2}, \quad (40)$$

with $p \neq q \neq j$ and $p, q, j = 1, 2, 3$.

The topological number of the BA stacking N -layer system is N times higher than that of the monolayer case and there is no phase transition by tuning t from zero to infinity. The TASP does not reflect the value of the topological number of the multilayer BA stacking system because the N layers of the structure overlap with each other in the

density plot in the Brillouin zone. However, they do reflect whether the system is topological. The exact value of the topological number for the N -layered system should be given by

$$w = \frac{N}{2\pi} \left(\int_{\mathcal{B}} \widetilde{\mathbf{g}} \cdot d\widetilde{\mathbf{g}} \right). \quad (41)$$

V. CONCLUSION

We have studied the dynamical characterization of topology in two types of layered systems, which are beyond the minimal models. We found that the term that anticommutes with all other terms still has the common BIS in this two layered systems. For the $AB - BA$ system, because of block diagonalization, in order to fully describe the topology, we need to redefine the BIS and observables for spin-texture fields in the subspaces, while for the BA system, the previous BIS and observables are still working. The condition for a term to have a BIS is relaxed into the following: If it is nonzero at all momentum values, it can keep the gap open for any deformation of the other terms. In addition, the magnitude of interlayer hopping can also be obtained from the TASP itself in these two stacking systems.

Since we studied two types of models and they share a similar dynamical characterization of the topology because of an anticommutation relation, it would be interesting to study whether we will have a general quench characterization of the topology for a Hamiltonian that does not have a term that anticommutes with all the other terms. For instance, for a Hamiltonian expanded by 3×3 Gell-Mann matrices satisfying SU(3) algebra, the characterization will be more complicated. Thus, it is interesting to see how the method of Liu and co-workers can be applied.

It was discussed in [19] that for models beyond the minimal models, it is possible to get a block-diagonalized form at each point in the Brillouin zone and then the BIS can be defined. However, our BA stacking model does not seem to fall into this category: From the dispersions (7) and (9), as long as t is not zero, they are not like the spectrum of $\sigma \cdot \mathbf{h}$ for some simple functions \mathbf{h} and thus cannot be block diagonalizable in most regions of the Brillouin zone.

ACKNOWLEDGMENTS

This work was supported by the National Key Research and Development Program of the Ministry of Science and Technology (Grant No. 2021 YFA1200700), the National Natural Science Foundation of China (Grant No. 12275075), and the Fundamental Research Funds for the Central Universities from China.

APPENDIX A: THE GTASP OF THE BILAYER AB - BA STACKING SYSTEM FOR THE TRIVIAL POSTQUENCH HAMILTONIAN

As plotted in Fig. 9, unlike the postquench Hamiltonian in the main text, which lies in a topological regime, the

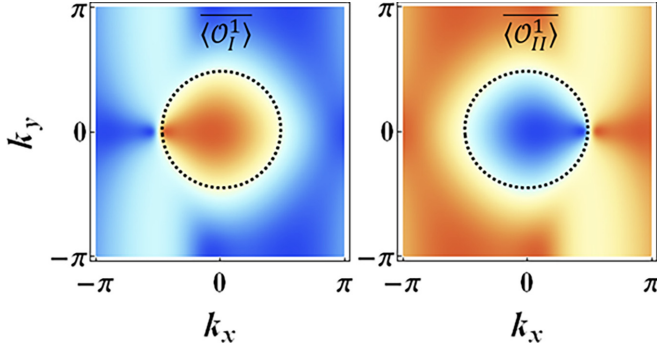


FIG. 9. Components of GTASPs $\langle \mathcal{O}_{I,II}^1 \rangle$. Here $m = 1$, $t = 1.2$, and $\rho_0 = \frac{1}{2} \otimes \frac{1}{2} (\mathbb{1} - \sigma_3)$.

components of GTASPs $\langle \mathcal{O}_{I,II}^1 \rangle$ for the trivial postquench Hamiltonian do not vanish on the line across the BIS.

APPENDIX B: THE TASP OF THE BILAYER BA STACKING SYSTEM FOR THE HALDANE MODEL

As shown in Fig. 10, we plot the TASP of the bilayer BA stacking system. The monolayer Hamiltonian describes the Haldane model and its effective fields are $h_1 = 4 \sum_{i=1}^3 \cos(\mathbf{k} \cdot \mathbf{a}_i)$, $h_2 = 4 \sum_{i=1}^3 \sin(\mathbf{k} \cdot \mathbf{a}_i)$, and $h_3 = m - 2 \sum_{i=1}^3 \sin(\mathbf{k} \cdot \mathbf{b}_i)$. Here $\mathbf{a}_1 = (0, 1)$, $\mathbf{a}_2 = (-\frac{\sqrt{3}}{2}, \frac{1}{2})$, $\mathbf{a}_3 = (\frac{\sqrt{3}}{2}, \frac{1}{2})$, $\mathbf{b}_1 = (-\sqrt{3}, 0)$, $\mathbf{b}_2 = (-\frac{\sqrt{3}}{2}, \frac{3}{2})$, and $\mathbf{b}_3 = (-\frac{\sqrt{3}}{2}, -\frac{3}{2})$. The parameter $m = 2\sqrt{3}$, which makes the postquench Hamiltonian lie in the topological regime. As we see, in each component of TASP, there exist three black dashed rings, on which all the components of TASP vanish. Thus, all three rings can be identified as BISs. Taking one BIS (upper right) as an example, we measure the dynamical field (arrows) on this BIS in the components of TASP $\langle \mathbb{1} \otimes \sigma_1 \rangle_{\rho_0}$ and $\langle \mathbb{1} \otimes \sigma_2 \rangle_{\rho_0}$, respectively, and then combine them into the component $\langle \mathbb{1} \otimes \sigma_3 \rangle_{\rho_0}$. The winding of the dynamical field on this BIS manifests a nontrivial topological phase, which implies the system lies in the topological phase. If the postquench Hamiltonian lies in the trivial regime, there is no BIS appearing in the TASP.

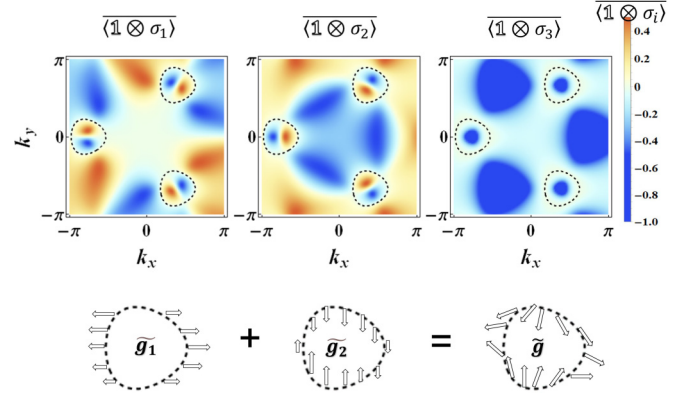


FIG. 10. The TASP and topological characterization of H_{BA}^2 . Here the monolayer Hamiltonian is from the Haldane model. The initial state ρ_0 is $\frac{1}{2} \otimes \frac{1}{2} (\mathbb{1} - \sigma_3)$. To show the dynamical field better, the combined field $\tilde{\mathbf{g}}$ is normalized. The interlayer hopping $t = 0.4$.

APPENDIX C: SPECTRA OF LAYERED SYSTEMS

1. The $AB - BA$ stacking system

The $AB - BA$ stacking bilayer model is defined by the Hamiltonian

$$H_{AB-BA}^2 := \begin{bmatrix} h_3 & h_1 - ih_2 & & t \\ h_1 + ih_2 & -h_3 & t & \\ & t & h_3 & h_1 - ih_2 \\ t & & h_1 + ih_2 & -h_3 \end{bmatrix} \\ = \sum_{i=1}^3 h_i \mathbb{1} \otimes \sigma_i + t \sigma_1 \otimes \sigma_1, \quad (\text{C1})$$

in which the anticommutation relations are

$$\{\mathbb{1} \otimes \sigma_i, \mathbb{1} \otimes \sigma_j\} = 2\mathbb{1} \otimes \delta_{ij}, \\ \{\mathbb{1} \otimes \sigma_2, \sigma_1 \otimes \sigma_1\} = 0, \\ \{\mathbb{1} \otimes \sigma_3, \sigma_1 \otimes \sigma_1\} = 0. \quad (\text{C2})$$

We block diagonalize this Hamiltonian to get two subsystems

$$H_{AB-BA}^2 ' = \frac{\mathbb{1} + i\sigma_2}{\sqrt{2}} \otimes \mathbb{1} H_{AB-BA}^2 \frac{\mathbb{1} - i\sigma_2}{\sqrt{2}} \otimes \mathbb{1} \\ = \frac{\mathbb{1} + i\sigma_2}{\sqrt{2}} \otimes \mathbb{1} \left(\sum_{i=1}^3 h_i \mathbb{1} \otimes \sigma_i + t \sigma_1 \otimes \sigma_1 \right) \frac{\mathbb{1} - i\sigma_2}{\sqrt{2}} \otimes \mathbb{1} \\ = \sum_{i=1}^3 h_i \mathbb{1} \otimes \sigma_i + t \sigma_3 \otimes \sigma_1 \\ = \begin{bmatrix} h_3 & h_1 + t - ih_2 & & \\ h_1 + t + ih_2 & -h_3 & & \\ & & h_3 & h_1 - t - ih_2 \\ & & h_1 - t + ih_2 & -h_3 \end{bmatrix} \\ =: H_I \oplus H_{II}. \quad (\text{C3})$$

Therefore, the spectrum is

$$E_I^\pm = \pm\sqrt{(h_1 + t)^2 + h_2^2 + h_3^2} = \pm E_I,$$

$$E_{II}^\pm = \pm\sqrt{(h_1 - t)^2 + h_2^2 + h_3^2} = \pm E_{II}. \quad (C4)$$

The multilayer $AB - BA$ stacking model has the Hamiltonian

$$H_{AB-BA}^N = \begin{bmatrix} \sum_{i=1}^3 h_i \sigma_i & t \sigma_1 & & & \\ t \sigma_1 & \sum_{i=1}^3 h_i & t \sigma_1 & & \\ & t \sigma_1 & \sum_{i=1}^3 h_i & \dots & \\ & & \dots & \dots & \dots \end{bmatrix}$$

$$= \sum_{i=1}^3 h_i \mathbb{1} \otimes \sigma_i + t \Sigma_1 \otimes \sigma_1, \quad (C5)$$

where

$$\Sigma_1 := \begin{bmatrix} 0 & 1 & 0 & 0 & \\ 1 & 0 & 1 & 0 & \\ 0 & 1 & 0 & 1 & \dots \\ 0 & 0 & 1 & 0 & \\ & & \dots & & \end{bmatrix} \quad (C6)$$

and the anticommutation relations are

$$\{\mathbb{1} \otimes \sigma_i, \mathbb{1} \otimes \sigma_j\} = 2\mathbb{1} \otimes \delta_{ij},$$

$$\{\mathbb{1} \otimes \sigma_2, \Sigma_1 \otimes \sigma_1\} = 0, \quad (C7)$$

$$\{\mathbb{1} \otimes \sigma_3, \Sigma_1 \otimes \sigma_1\} = 0.$$

To block diagonalize H_{AB-BA}^N , we just need to diagonalize Σ_1 , which is given by

$$\Sigma'_1 = S_{\Sigma_1}^{-1} \Sigma_1 S_{\Sigma_1} = \begin{bmatrix} 2 \cos \theta_1 & & & & \\ & 2 \cos \theta_2 & & & \\ & & \dots & & \\ & & & \dots & \\ & & & & 2 \cos \theta_N \end{bmatrix}, \quad (C8)$$

where

$$S_{\Sigma_1} = (\mathbf{a}_1, \mathbf{a}_2, \dots, \mathbf{a}_N),$$

$$\mathbf{a}_r = \sqrt{\frac{2}{N+1}} (\sin \theta_r, \sin 2\theta_r, \dots, \sin N\theta_r)^T,$$

$$\theta_r = \frac{r\pi}{N+1}, \quad r = 1, 2, \dots, N. \quad (C9)$$

Therefore, the block-diagonalized Hamiltonian is

$$H_{AB-BA}^{N'} =: \bigoplus_{r=1}^n H_r, \quad (C10)$$

where

$$H_r = \sum_{i=1}^3 h_i \sigma_i - 2t \cos \theta_r, \quad (C11)$$

and the spectrum is

$$E_r^\pm = \pm\sqrt{(h_1 - 2t \cos \theta_r)^2 + h_2^2 + h_3^2} = \pm E_r,$$

$$r = 1, 2, \dots, N. \quad (C12)$$

2. The BA stacking system

The bilayer BA stacking model is defined by the Hamiltonian

$$H_{BA}^2 = \begin{bmatrix} h_3 & h_1 - ih_2 & & & \\ h_1 + ih_2 & -h_3 & t & & \\ & t & h_3 & h_1 - ih_2 & \\ & & h_1 + ih_2 & -h_3 & \end{bmatrix}$$

$$= \sum_{i=1}^3 h_i \mathbb{1} \otimes \sigma_i + \frac{t}{2} (\sigma_1 \otimes \sigma_1 + \sigma_2 \otimes \sigma_2), \quad (C13)$$

in which the anticommutation relations are

$$\{\mathbb{1} \otimes \sigma_i, \mathbb{1} \otimes \sigma_j\} = 2\mathbb{1} \otimes \delta_{ij},$$

$$\{\mathbb{1} \otimes \sigma_3, \sigma_1 \otimes \sigma_1\} = 0,$$

$$\{\mathbb{1} \otimes \sigma_3, \sigma_2 \otimes \sigma_2\} = 0. \quad (C14)$$

The spectrum is

$$E_1^+ = \sqrt{h_3^2 + \left[\sqrt{\left(\frac{t}{2}\right)^2 + h_1^2 + h_2^2} + \frac{t}{2} \right]^2},$$

$$E_2^+ = \sqrt{h_3^2 + \left[\sqrt{\left(\frac{t}{2}\right)^2 + h_1^2 + h_2^2} - \frac{t}{2} \right]^2},$$

$$E_2^- = -\sqrt{h_3^2 + \left[\sqrt{\left(\frac{t}{2}\right)^2 + h_1^2 + h_2^2} - \frac{t}{2} \right]^2},$$

$$E_1^- = -\sqrt{h_3^2 + \left[\sqrt{\left(\frac{t}{2}\right)^2 + h_1^2 + h_2^2} + \frac{t}{2} \right]^2},$$

$$E_1^+ \geq E_2^+ > E_2^- \geq E_1^-. \quad (C15)$$

All the eigenenergies satisfy

$$\left(E_m^2 - \sum_i h_i^2 \right)^2 = t^2 (E_m^2 - h_3^2)^2, \quad (C16)$$

so the eigenvectors can be written as

$$|\psi_m\rangle = \begin{pmatrix} t(h_1 - ih_2)(E_m + h_3) \\ t(E_m^2 - h_3^2) \\ (E_m^2 - \sum_i h_i^2)(E_m + h_3) \\ (E_m^2 - \sum_i h_i^2)(h_1 + ih_2) \end{pmatrix} \quad (C17)$$

and the normalization is

$$\langle \psi_m | \psi_m \rangle = 2t^2 E_m (E_m + h_3) (E_m^2 - h_3^2 + h_1^2 + h_2^2).$$

Then we have

$$\langle \tilde{\psi}_m | \mathbb{1} \otimes \sigma_1 | \tilde{\psi}_m \rangle = \frac{2h_1 (E_m^2 - h_3^2)}{E_m (E_m^2 - h_3^2 + h_1^2 + h_2^2)}, \quad (C18)$$

$$\langle \tilde{\psi}_m | \mathbb{1} \otimes \sigma_2 | \tilde{\psi}_m \rangle = \frac{2h_2 (E_m^2 - h_3^2)}{E_m (E_m^2 - h_3^2 + h_1^2 + h_2^2)} \quad (C19)$$

and $\langle \tilde{\psi}_m | \mathbb{1} \otimes \sigma_3 | \tilde{\psi}_m \rangle$ is calculated in Eq. (E4).

APPENDIX D: DENSITY MATRICES OF THE INITIAL STATES

We choose the prequench Hamiltonian by taking, for instance, h_i to be positive infinity so that

$$H_P \rightarrow h_i \mathbb{1} \otimes \sigma_i \quad (\text{no summation over } i). \quad (\text{D1})$$

Considering bilayer models for simplicity, we have the eigenequation

$$\begin{pmatrix} h_i \sigma_i - E_{\pm} & 0 \\ 0 & h_i \sigma_i - E_{\pm} \end{pmatrix} \begin{pmatrix} \xi_{\pm} \\ \eta_{\pm} \end{pmatrix} = 0, \quad (\text{D2})$$

with solutions

$$\begin{aligned} E_{\pm} &= \pm h_i, \\ \xi_{\pm} \xi_{\pm}^{\dagger} &= |c_1|^2 \frac{\mathbb{1} \pm \sigma_i}{2}, \\ \eta_{\pm} \eta_{\pm}^{\dagger} &= |c_2|^2 \frac{\mathbb{1} \pm \sigma_i}{2}, \\ |c_1|^2 + |c_2|^2 &= 1. \end{aligned} \quad (\text{D3})$$

So a pure initial state has the density matrix

$$\begin{aligned} \rho_{\pm}^p &= \begin{pmatrix} \xi_{\pm} \\ \eta_{\pm} \end{pmatrix} \begin{pmatrix} \xi_{\pm} \\ \eta_{\pm} \end{pmatrix}^{\dagger} \\ &= \begin{pmatrix} c_1 \\ c_2 \end{pmatrix} \begin{pmatrix} c_1^* & c_2^* \end{pmatrix} \otimes \frac{\mathbb{1} \pm \sigma_i}{2}, \end{aligned} \quad (\text{D4})$$

while a mixed density matrix containing half $\begin{pmatrix} \xi_{\pm} \\ 0 \end{pmatrix}$ and half $\begin{pmatrix} 0 \\ \eta_{\pm} \end{pmatrix}$ is

$$\begin{aligned} \rho_{\pm}^m &= \frac{1}{2} \begin{pmatrix} \xi_{\pm} \\ 0 \end{pmatrix} \begin{pmatrix} \xi_{\pm} \\ 0 \end{pmatrix}^{\dagger} + \frac{1}{2} \begin{pmatrix} 0 \\ \eta_{\pm} \end{pmatrix} \begin{pmatrix} 0 \\ \eta_{\pm} \end{pmatrix}^{\dagger} \\ &= \frac{\mathbb{1}}{2} \otimes \frac{\mathbb{1} \pm \sigma_i}{2}. \end{aligned} \quad (\text{D5})$$

APPENDIX E: DERIVATION OF THE COMMON BIS

The TASP for any Hamiltonian can be written as

$$\begin{aligned} \overline{\langle \mathbb{1} \otimes \sigma_i \rangle_{\rho_0}} &= \lim_{T \rightarrow \infty} \frac{1}{T} \int_0^T dt \text{Tr}(\rho_0 e^{iHt} \mathbb{1} \otimes \sigma_i e^{-iHt}) \\ &= \sum_m \langle \tilde{\psi}_m | \rho_0 | \tilde{\psi}_m \rangle \langle \tilde{\psi}_m | \mathbb{1} \otimes \sigma_i | \tilde{\psi}_m \rangle. \end{aligned} \quad (\text{E1})$$

If a Hamiltonian has the property

$$H = H_0 + h_3 \mathbb{1} \otimes \sigma_3, \quad (\text{E2})$$

$$\langle H_0, h_3 \mathbb{1} \otimes \sigma_3 \rangle = 0, \quad (\text{E3})$$

then

$$\langle \tilde{\psi}_m | \mathbb{1} \otimes \sigma_3 | \tilde{\psi}_m \rangle = h_3 / E_m, \quad (\text{E4})$$

where $|\tilde{\psi}_m\rangle$ is the normalized eigenvector, E_m is the eigenvalue of H , and the index m represents indices r and \pm . This is because, on the one hand,

$$\begin{aligned} \langle \tilde{\psi}_m | \{H, \mathbb{1} \otimes \sigma_3\} | \tilde{\psi}_m \rangle &= \langle \tilde{\psi}_m | \{h_3 \mathbb{1} \otimes \sigma_3, \mathbb{1} \otimes \sigma_3\} | \tilde{\psi}_m \rangle \\ &= 2h_3, \end{aligned} \quad (\text{E5})$$

and, on the other hand,

$$\langle \tilde{\psi}_m | \{H, \mathbb{1} \otimes \sigma_3\} | \tilde{\psi}_m \rangle = 2E_m \langle \tilde{\psi}_m | \mathbb{1} \otimes \sigma_3 | \tilde{\psi}_m \rangle. \quad (\text{E6})$$

Substituting Eqs. (E4) and (D5) into Eq. (E1), we get

$$\overline{\langle \mathbb{1} \otimes \sigma_i \rangle_{\rho_0}} = -h_3 \sum_m \frac{\langle \tilde{\psi}_m | \mathbb{1} \otimes \sigma_i | \tilde{\psi}_m \rangle}{4E_m}. \quad (\text{E7})$$

Note that if we choose a pure state like Eq. (D4), in general, we will not get a form like

$$\overline{\langle \mathbb{1} \otimes \sigma_i \rangle_{\rho_0}} \propto -h_3, \quad (\text{E8})$$

so it is important that the initial state is chosen as Eq. (D5).

APPENDIX F: CALCULATION OF TIME-AVERAGED SPIN POLARIZATION

1. The $AB - BA$ system

First, we calculate the TASP in the bilayer case. Using Eqs. (E4) and (E1), we calculate

$$\begin{aligned} \overline{\langle \mathbb{1} \otimes \sigma_i \rangle_{\rho_0}} &= \lim_{T \rightarrow \infty} \frac{1}{T} \int_0^T dt \text{Tr}(\rho_0 e^{iH_{AB-BA}^2 t} \mathbb{1} \otimes \sigma_i e^{-iH_{AB-BA}^2 t}) \\ &= \lim_{T \rightarrow \infty} \frac{1}{T} \int_0^T dt \text{Tr}(S \rho_0 S^{-1} e^{iS H_{AB-BA}^2 S^{-1} t} S \mathbb{1} \\ &\quad \otimes \sigma_i S^{-1} e^{-iS H_{AB-BA}^2 S^{-1} t}) \\ &= \lim_{T \rightarrow \infty} \frac{1}{T} \int_0^T dt \text{Tr}(\rho_0 e^{iH_{AB-BA}^2 t} \mathbb{1} \otimes \sigma_i e^{-iH_{AB-BA}^2 t}) \end{aligned} \quad (\text{F1})$$

$$\begin{aligned} &= \lim_{T \rightarrow \infty} \frac{1}{T} \int_0^T dt \text{Tr}(\rho_0^I e^{iH_{II} t} \sigma_i e^{-iH_{II} t} \\ &\quad + \rho_0^J e^{iH_{II} t} \sigma_i e^{-iH_{II} t}) \\ &= -\frac{h_I^j h_I^j}{2E_I^2} - \frac{h_{II}^j h_{II}^j}{2E_{II}^2}, \end{aligned} \quad (\text{F2})$$

where we use

$$S = \frac{\mathbb{1} + i\sigma_2}{\sqrt{2}} \otimes \mathbb{1},$$

$$\begin{aligned} S \rho_0 S^{-1} &= \frac{\mathbb{1} + i\sigma_2}{\sqrt{2}} \otimes \mathbb{1} \left(\frac{\mathbb{1}}{2} \otimes \frac{1}{2} (\mathbb{1} - \sigma_j) \right) \frac{\mathbb{1} - i\sigma_2}{\sqrt{2}} \otimes \mathbb{1} \\ &= \rho_0, \end{aligned}$$

$$\rho_0 = \frac{\mathbb{1} - \sigma_j}{4} \oplus \frac{\mathbb{1} + \sigma_j}{4} = \rho_0^I \oplus \rho_0^{II}, \quad (\text{F3})$$

$$h_I^j = h_1 + t, \quad h_{II}^j = h_1 - t, \quad (\text{F4})$$

$$h_I^2 = h_2, \quad h_I^3 = h_3, \quad h_{II}^2 = h_2, \quad h_{II}^3 = h_3. \quad (\text{F5})$$

The H_{AB-BA}^2 can be block diagonalized by the transformation S , so we will take advantage of this to organize the quench process as well. In order to set them apart, we consider the operators \mathcal{O}_I^j and \mathcal{O}_{II}^j to obtain

$$\overline{\langle \mathcal{O}_I^j \rangle_{\rho_0}} = -\frac{h_I^j h_I^j}{2E_I^2}, \quad (\text{F6})$$

$$\overline{\langle \mathcal{O}_{II}^j \rangle_{\rho_0}} = -\frac{h_{II}^j h_{II}^j}{2E_{II}^2}. \quad (\text{F7})$$

This can be done by considering the two subspaces of $\mathbb{1} \otimes \sigma_i$ in Eq. (F1), $(\begin{smallmatrix} 1 & \\ & 0 \end{smallmatrix}) \otimes \sigma_i$ and $(\begin{smallmatrix} 0 & \\ & 1 \end{smallmatrix}) \otimes \sigma_i$, such that

$$S\mathcal{O}_I^i S^{-1} = \begin{pmatrix} 2 & \\ & 0 \end{pmatrix} \otimes \sigma_i, \quad (\text{F8})$$

$$S\mathcal{O}_{II}^i S^{-1} = \begin{pmatrix} 0 & \\ & 2 \end{pmatrix} \otimes \sigma_i. \quad (\text{F9})$$

These equations can be solved by

$$\mathcal{O}_I^i = (\mathbb{1} + \sigma_1) \otimes \sigma_i, \quad (\text{F10})$$

$$\mathcal{O}_{II}^i = (\mathbb{1} - \sigma_1) \otimes \sigma_i. \quad (\text{F11})$$

Second, we calculate the TASP in the multilayer case

$$\begin{aligned} \overline{\langle \mathbb{1} \otimes \sigma_i \rangle}_{\rho_0} &= \lim_{T \rightarrow \infty} \frac{1}{T} \int_0^T dt \text{Tr}(\rho_0 e^{iH_{AB-BA}^n t} \mathbb{1} \otimes \sigma_i e^{-iH_{AB-BA}^n t}) \\ &= \lim_{T \rightarrow \infty} \frac{1}{T} \int_0^T dt \text{Tr}(S\rho_0 S^{-1} e^{iSH_{AB-BA}^n S^{-1} t} S\mathbb{1} \\ &\quad \otimes \sigma_i S^{-1} e^{-iSH_{AB-BA}^n S^{-1} t}) \\ &= \lim_{T \rightarrow \infty} \frac{1}{T} \int_0^T dt \text{Tr}(\rho_0 e^{iH_{AB-BA}^n t} \mathbb{1} \otimes \sigma_i e^{-iH_{AB-BA}^n t}) \end{aligned} \quad (\text{F12})$$

$$\begin{aligned} &= \lim_{T \rightarrow \infty} \frac{1}{T} \int_0^T dt \text{Tr} \left(\sum_{r=1}^n \rho_0^r e^{iH_r t} \sigma_i e^{-iH_r t} \right) \\ &= - \sum_{r=1}^n \frac{h_r^i h_r^j}{2E_r^2}, \end{aligned} \quad (\text{F13})$$

where we use

$$S\rho_0 S^{-1} = \rho_0, \quad S = S_{\Sigma_1} \otimes \mathbb{1}, \quad (\text{F14})$$

$$\rho_0 = \bigoplus_{r=1}^N \rho_0^r, \quad \rho_0^r = \frac{\mathbb{1} - \sigma_j}{2N}, \quad (\text{F15})$$

$$h_r^1 = h_1 - 2t \cos \theta_r, \quad (\text{F16})$$

$$h_r^2 = h_2, \quad h_r^3 = h_3. \quad (\text{F17})$$

In order to set them apart, we consider the operators \mathcal{O}_r such that

$$\overline{\langle \mathcal{O}_r^i \rangle}_{\rho_0} = - \frac{h_r^i h_r^j}{E_r^2}. \quad (\text{F18})$$

This can be done by considering the N subspaces of $\mathbb{1} \otimes \sigma_i$ in Eq. (F1) such that

$$S\mathcal{O}_r^i S^{-1} = \underbrace{(\mathbf{0} \oplus \dots \oplus \mathbf{0})}_{r-1 \mathbf{0}s} \oplus \mathbb{1}_2 \oplus \mathbf{0} \oplus \dots \oplus \mathbf{0} \otimes \sigma_i, \quad (\text{F19})$$

which is solved by

$$\mathcal{O}_r^i = \mathbf{a}_r \mathbf{a}_r^T \otimes \sigma_i. \quad (\text{F20})$$

The \mathbf{a}_r is defined in Eq. (C9).

2. The BA system

From Eqs. (E1), (C18), and (C19), for the bilayer system, the components of TASP are

$$\begin{aligned} \overline{\langle \mathbb{1} \otimes \sigma_1 \rangle}_{\rho_0} &= -h_1 h_3 \sum_m \frac{E_m^2 - h_3^2}{2E_m^2 (E_m^2 - h_3^2 + h_1^2 + h_2^2)}, \\ \overline{\langle \mathbb{1} \otimes \sigma_2 \rangle}_{\rho_0} &= -h_2 h_3 \sum_m \frac{E_m^2 - h_3^2}{2E_m^2 (E_m^2 - h_3^2 + h_1^2 + h_2^2)}, \quad (\text{F21}) \\ \overline{\langle \mathbb{1} \otimes \sigma_3 \rangle}_{\rho_0} &= -h_3^2 \sum_m \frac{1}{4E_m^2}, \end{aligned}$$

in which the initial state

$$\rho_0 = \frac{\mathbb{1}}{2} \otimes \frac{\mathbb{1}}{2} (\mathbb{1} - \sigma_3).$$

For the initial state

$$\rho_0 = \frac{\mathbb{1}}{2} \otimes \frac{\mathbb{1}}{2} (\mathbb{1} - \sigma_a), \quad a = 1, 2,$$

the components of TASP are

$$\begin{aligned} \overline{\langle \mathbb{1} \otimes \sigma_1 \rangle}_{\rho_0} &= -h_1 h_a \sum_m \frac{(E_m^2 - h_3^2)^2}{E_m^2 (E_m^2 - h_3^2 + h_1^2 + h_2^2)^2}, \\ \overline{\langle \mathbb{1} \otimes \sigma_2 \rangle}_{\rho_0} &= -h_2 h_a \sum_m \frac{(E_m^2 - h_3^2)^2}{E_m^2 (E_m^2 - h_3^2 + h_1^2 + h_2^2)^2}, \quad (\text{F22}) \\ \overline{\langle \mathbb{1} \otimes \sigma_3 \rangle}_{\rho_0} &= -h_3 h_a \sum_m \frac{E_m^2 - h_3^2}{2E_m^2 (E_m^2 - h_3^2 + h_1^2 + h_2^2)}. \end{aligned}$$

In short, we have

$$\overline{\langle \mathbb{1} \otimes \sigma_i \rangle}_{\rho_0} = -h_i h_j A_{ij} \quad (\text{no summation over } i, j), \quad (\text{F23})$$

$$\rho_0 = \frac{\mathbb{1}}{2} \otimes \frac{\mathbb{1}}{2} (\mathbb{1} - \sigma_j), \quad (\text{F24})$$

$$A_{11} = A_{12} = A_{21} = A_{22} = \sum_m \frac{(E_m^2 - h_3^2)^2}{E_m^2 (E_m^2 - h_3^2 + h_1^2 + h_2^2)^2}, \quad (\text{F25})$$

$$A_{13} = A_{31} = A_{23} = A_{32} = \sum_m \frac{E_m^2 - h_3^2}{2E_m^2 (E_m^2 - h_3^2 + h_1^2 + h_2^2)}, \quad (\text{F26})$$

$$A_{33} = \sum_m \frac{1}{4E_m^2}. \quad (\text{F27})$$

Let us look at the dynamical spin-texture fields

$$\widetilde{g}_i(\mathbf{k}) = -\frac{1}{\mathcal{N}_{\mathbf{k}}} \partial_{k_\perp} \overline{\langle \mathbb{1} \otimes \sigma_i \rangle}_{\rho_0}. \quad (\text{F28})$$

For the initial state

$$\rho_0 = \frac{\mathbb{1}}{2} \otimes \frac{\mathbb{1}}{2} (\mathbb{1} - \sigma_3),$$

whose BIS is at $h_3 = 0$, the difference is calculated as

$$\begin{aligned} \Delta \overline{\langle \mathbb{1} \otimes \sigma_a \rangle}_{\rho_0} \Big|_{k_{\perp} \rightarrow 0} &= - \left[\left(h_a h_3 \sum_m \frac{E_m^2 - h_3^2}{2E_m^2(E_m^2 - h_3^2 + h_1^2 + h_2^2)} \right) \Big|_{(k_{\perp}, \mathbf{k}_{\parallel})} - \left(h_a h_3 \sum_m \frac{E_m^2 - h_3^2}{2E_m^2(E_m^2 - h_3^2 + h_1^2 + h_2^2)} \right) \Big|_{(-k_{\perp}, \mathbf{k}_{\parallel})} \right] \Big|_{k_{\perp} \rightarrow 0} \\ &\propto - \left(2h_a k_{\perp} \sum_m \frac{E_m^2 - h_3^2}{2E_m^2(E_m^2 - h_3^2 + h_1^2 + h_2^2)} \right) \Big|_{(0, \mathbf{k}_{\parallel})}, \end{aligned} \quad (\text{F29})$$

with $a = 1, 2$. After normalization, we get

$$\widetilde{g_a(\mathbf{k})} \Big|_{\mathbf{k} \in \text{BIS}} = \frac{h^a(0, \mathbf{k}_{\parallel})}{\sum_{a=1}^2 [h^a(0, \mathbf{k}_{\parallel})]^2} = \hat{h}^{so,a}. \quad (\text{F30})$$

For the initial state

$$\rho_0 = \frac{\mathbb{1}}{2} \otimes \frac{1}{2}(\mathbb{1} - \sigma_a), \quad a = 1, 2,$$

whose BIS is at $h_a = 0$, the difference is calculated as

$$\begin{aligned} \Delta \overline{\langle \mathbb{1} \otimes \sigma_b \rangle}_{\rho_0} \Big|_{k_{\perp} \rightarrow 0} &\propto -2h_b k_{\perp} \sum_m \frac{(E_m^2 - h_3^2)^2}{E_m^2(E_m^2 - h_3^2 + h_1^2 + h_2^2)^2} \Big|_{(0, \mathbf{k}_{\parallel})}, \quad b = 1, 2, \\ \Delta \overline{\langle \mathbb{1} \otimes \sigma_3 \rangle}_{\rho_0} \Big|_{k_{\perp} \rightarrow 0} &\propto -2h_3 k_{\perp} \sum_m \frac{E_m^2 - h_3^2}{2E_m^2(E_m^2 - h_3^2 + h_1^2 + h_2^2)} \Big|_{(0, \mathbf{k}_{\parallel})}. \end{aligned} \quad (\text{F31})$$

In short, for

$$\begin{aligned} \rho_0 &= \frac{\mathbb{1}}{2} \otimes \frac{1}{2}(\mathbb{1} - \sigma_j), \quad j = 1, 2, 3, \\ \Delta \overline{\langle \mathbb{1} \otimes \sigma_i \rangle}_{\rho_0} \Big|_{k_{\perp} \rightarrow 0} &\propto -2(A_{ij} h_i) \Big|_{(0, \mathbf{k}_{\parallel})} k_{\perp}. \end{aligned} \quad (\text{F32})$$

Thus

$$\begin{aligned} \widetilde{g_p(\mathbf{k})} \Big|_{\mathbf{k} \in \mathcal{B}} &= \frac{A_{pj} h_p}{(A_{pj} h_p)^2 + (A_{qj} h_q)^2}, \\ p \neq q \neq j; \quad p, q, j &= 1, 2, 3. \end{aligned} \quad (\text{F33})$$

Here $\tilde{\mathbf{g}}$ is a vector with two components.

Next we consider N -layer BA systems. The components of TASP are

$$\begin{aligned} \overline{\langle \mathbb{1} \otimes \sigma_1 \rangle}_{\rho_0} &= -h_1 h_3 \sum_m \frac{E_m^2 - h_3^2}{ND_m}, \\ \overline{\langle \mathbb{1} \otimes \sigma_2 \rangle}_{\rho_0} &= -h_2 h_3 \sum_m \frac{E_m^2 - h_3^2}{ND_m}, \\ \overline{\langle \mathbb{1} \otimes \sigma_3 \rangle}_{\rho_0} &= -h_3^2 \sum_m \frac{1}{2NE_m^2}, \end{aligned} \quad (\text{F34})$$

with the initial state

$$\rho_0 = \frac{\mathbb{1}}{N} \otimes \frac{1}{2}(\mathbb{1} - \sigma_3).$$

For the initial state

$$\rho_0 = \frac{\mathbb{1}}{N} \otimes \frac{1}{2}(\mathbb{1} - \sigma_a), \quad a = 1, 2,$$

the components of TASP are

$$\begin{aligned} \overline{\langle \mathbb{1} \otimes \sigma_1 \rangle}_{\rho_0} &= -h_1 h_a \sum_m \frac{2(E_m^2 - h_3^2)^2}{N^2 D_m^2}, \\ \overline{\langle \mathbb{1} \otimes \sigma_2 \rangle}_{\rho_0} &= -h_2 h_a \sum_m \frac{2(E_m^2 - h_3^2)^2}{N^2 D_m^2}, \\ \overline{\langle \mathbb{1} \otimes \sigma_3 \rangle}_{\rho_0} &= -h_3 h_a \sum_m \frac{E_m^2 - h_3^2}{ND_m}, \end{aligned} \quad (\text{F35})$$

where

$$\begin{aligned} D_m &= E_m \left(E_m(E_m^2 - h_3^2 + h_1^2 + h_2^2) \right. \\ &\quad \left. - \frac{1 + (-1)^{N+1}}{N+1} h_3(E_m^2 - h_3^2 - h_1^2 - h_2^2) \right). \end{aligned} \quad (\text{F36})$$

In short, we have

$$\overline{\langle \mathbb{1} \otimes \sigma_i \rangle}_{\rho_0} = -h_i h_j A_{ij}^{(N)} \quad (\text{no summation over } i, j), \quad (\text{F37})$$

$$\rho_0 = \frac{\mathbb{1}}{2} \otimes \frac{1}{2}(\mathbb{1} - \sigma_j), \quad (\text{F38})$$

$$A_{11}^{(N)} = A_{12}^{(N)} = A_{21}^{(N)} = A_{22}^{(N)} = \sum_m \frac{2(E_m^2 - h_3^2)^2}{D_m^2}, \quad (\text{F39})$$

$$A_{13}^{(N)} = A_{31}^{(N)} = A_{23}^{(N)} = A_{32}^{(N)} = \sum_m \frac{E_m^2 - h_3^2}{D_m}, \quad (\text{F40})$$

$$A_{33}^{(N)} = \sum_m \frac{1}{2NE_m^2}. \quad (\text{F41})$$

Like the bilayer case, for the initial state

$$\begin{aligned} \rho_0 &= \frac{\mathbb{1}}{2} \otimes \frac{1}{2}(\mathbb{1} - \sigma_j), \\ j = 1, 2, 3, \Delta \langle \mathbb{1} \otimes \sigma_i \rangle_{\rho_0} \Big|_{k_\perp \rightarrow 0} &\propto -2(A_{ij}^{(N)} h_i) \Big|_{(0, \mathbf{k}_\parallel)} k_\perp \end{aligned} \quad (\text{F42})$$

and

$$\widetilde{g}_p(\mathbf{k}) \Big|_{\mathbf{k} \in \mathcal{B}} = \frac{A_{pj}^{(N)} h_p}{(A_{pj}^{(N)} h_p)^2 + (A_{qj}^{(N)} h_q)^2}, \quad p \neq q \neq j; \\ p, q, j = 1, 2, 3.$$

Here $\widetilde{\mathbf{g}}$ is a vector with two components.

-
- [1] M. Z. Hasan and C. L. Kane, *Rev. Mod. Phys.* **82**, 3045 (2010).
- [2] X. L. Qi and S.-C. Zhang, *Rev. Mod. Phys.* **83**, 1057 (2011).
- [3] Y. Hatsugai, *Phys. Rev. Lett.* **71**, 3697 (1993).
- [4] X.-G. Wen, *Quantum Field Theory of Many-Body Systems: From the Origin of Sound to an Origin of Light and Electrons* (Oxford University Press, Oxford, 2004).
- [5] W. A. Benalcazar, B. A. Bernevig, and T. L. Hughes, *Science* **357**, 61 (2017).
- [6] F. Schindler, A. M. Cook, M. G. Vergniory, Z. Wang, S. S. P. Parkin, B. A. Bernevig, and T. Neupert, *Sci. Adv.* **4**, eaat0346 (2018).
- [7] M. D. Caio, N. R. Cooper, and M. J. Bhaseen, *Phys. Rev. Lett.* **115**, 236403 (2015).
- [8] Y. Hu, P. Zoller, and J. C. Budich, *Phys. Rev. Lett.* **117**, 126803 (2016).
- [9] C. Wang, P. Zhang, X. Chen, J. Yu, and H. Zhai, *Phys. Rev. Lett.* **118**, 185701 (2017).
- [10] H. Hu and E. Zhao, *Phys. Rev. Lett.* **124**, 160402 (2020).
- [11] M. McGinley and N. R. Cooper, *Phys. Rev. B* **99**, 075148 (2019).
- [12] X. Chen, C. Wang, and J. Yu, *Phys. Rev. A* **101**, 032104 (2020).
- [13] N. Fläschner, D. Vogel, M. Tarnowski, B. S. Rem, D.-S. Lühmann, M. Heyl, J. C. Budich, L. Mathey, K. Sengstock, and C. Weitenberg, *Nat. Phys.* **14**, 265 (2018).
- [14] B. Song, L. Zhang, C. He, T. F. J. Poon, E. Hajiyev, S. Zhang, X.-J. Liu, and G.-B. Jo, *Sci. Adv.* **4**, eaao4748 (2018).
- [15] W. Sun, C.-R. Yi, B.-Z. Wang, W.-W. Zhang, B. C. Sanders, X.-T. Xu, Z.-Y. Wang, J. Schmiedmayer, Y. Deng, X.-J. Liu, S. Chen, and J.-W. Pan, *Phys. Rev. Lett.* **121**, 250403 (2018).
- [16] B. Song, C. He, S. Niu, L. Zhang, Z. Ren, X.-J. Liu, and G.-B. Jo, *Nat. Phys.* **15**, 911 (2019).
- [17] T. Xin, Y. Li, Y.-A. Fan, X. Zhu, Y. Zhang, X. Nie, J. Li, Q. Liu, and D. Lu, *Phys. Rev. Lett.* **125**, 090502 (2020).
- [18] J. Niu, T. Yan, Y. Zhou, Z. Tao, X. Li, W. Liu, L. Zhang, H. Jia, S. Liu, Z. Yan, Y. Chen, D. Yu, and J. Du, *Sci. Bull.* **66**, 1168 (2021).
- [19] L. Zhang, L. Zhang, S. Niu, and X.-J. Liu, *Sci. Bull.* **63**, 1385 (2018).
- [20] L. Zhang, L. Zhang, and X.-J. Liu, *Phys. Rev. A* **99**, 053606 (2019).
- [21] X.-L. Yu, W. Ji, L. Zhang, Y. Wang, J. Wu, and X.-J. Liu, *PRX Quantum* **2**, 020320 (2021).
- [22] Y. Wang, W. Ji, Z. Chai, Y. Guo, M. Wang, X. Ye, P. Yu, L. Zhang, X. Qin, P. Wang, F. Shi, X. Rong, D. Lu, X.-J. Liu, and J. Du, *Phys. Rev. A* **100**, 052328 (2019).
- [23] C.-R. Yi, L. Zhang, L. Zhang, R.-H. Jiao, X.-C. Cheng, Z.-Y. Wang, X.-T. Xu, W. Sun, X.-J. Liu, S. Chen, and J.-W. Pan, *Phys. Rev. Lett.* **123**, 190603 (2019).
- [24] L. Zhang, L. Zhang, and X.-J. Liu, *Phys. Rev. Lett.* **125**, 183001 (2020).
- [25] L. Li, W. Zhu, and J. Gong, *Sci. Bull.* **66**, 1502 (2021).
- [26] W. P. Su, J. R. Schrieffer, and A. J. Heeger, *Phys. Rev. Lett.* **42**, 1698 (1979).
- [27] F. D. M. Haldane, *Phys. Rev. Lett.* **61**, 2015 (1988).
- [28] Z. Lei, Y. Deng, and L. Li, *Phys. Rev. B* **106**, 245105 (2022).
- [29] H. Min and A. H. MacDonald, *Phys. Rev. B* **77**, 155416 (2008).
- [30] H. Min and A. H. MacDonald, *Prog. Theor. Phys. Suppl.* **176**, 227 (2008).
- [31] R. Yu, W. Zhang, H.-J. Zhang, S.-C. Zhang, X. Dai, and Z. Fang, *Science* **329**, 61 (2010).
- [32] K. Hashimoto and T. Kimura, *Prog. Theor. Exp. Phys.* **2016**, 013B04 (2016).
- [33] X.-L. Qi, Y.-S. Wu, and S.-C. Zhang, *Phys. Rev. B* **74**, 085308 (2006).
- [34] X. Wu, *arXiv:2302.00307*.